

Linearized Extended Waveform Inversion

Yin Huang, William Symes, Rice University

SUMMARY

The extended model concept links migration velocity analysis and waveform inversion. This abstract presents a method to solve a partially linearized version of the full waveform inversion problem with model extension. Linearization separates the model of the earth into the smooth long scale background model and the short scale model. Extended waveform inversion allows the short scale model to depend on an extra parameter, for example the shot coordinates. The objective function is the least squares misfit function of Born modeling, plus a differential semblance term. Minimization over the short scale model (a quadratic problem) by an iterative method results in a smooth objective function over the background model. Computation of objective values from Marmousi model with acoustic constant density modeling illustrate the smoothness and unimodality of the objective, for proper choice of parameters.

INTRODUCTION

Seismic reflection inversion is over-determined in the sense that multiple shot gathers need to be fitted simultaneously. A localized change in wave velocity sufficient to induce a travel-time shift by a wavelength along some ray paths typically affects the data fit for some shots but not for others, and may generate spuriously good local fits (“cycle skipping”). Thus the least-squares data fitting function has many local minima far from its global minimum (Gauthier et al., 1986; Santosa and Symes, 1989; Virieux and Operto, 2009). The density of local minima increases, and the size of the basin of attraction of each local minimum decreases, as the central frequency of the data increases. That is, the least squares objective function is not stable with respect to data frequency content, as is well known (Jannane et al., 1989).

If we fit a different model to each shot, the least squares objective becomes much easier to drive to a global minimizer. A shot-dependent model is not physical, of course; it is an example of an *extended model*. There are many other types of extension (ways of introducing nonphysical degrees of freedom into the model parameters). Inversion for a shot-dependent model (or any extension) by data fitting is underdetermined. An extra constraint must be imposed to suppress the nonphysical degrees of freedom, and thus recover some control over the model estimate.

The primary aim of this abstract is to explain *how* smooth objective functions of model parameters arise from data misfit and extended modeling, augmented with a particular type of constraint, and use numerical results to illustrate the smoothness of these functions, with carefully chosen parameters.

We will limit our discussion to linearized extended model-

ing, in which the model is split into long-scale components (the macro-model) and short-scale components (the reflectivity). Only the short-scale components are extended (allowed to depend on parameters other than spatial coordinates). The predicted data is modeled via linearization (Born approximation), viewing the short-scale components as perturbation about the long-scale model. While inversion based on full wave extended modeling has been studied by a number of authors (Symes, 1986, 1991; Biondi and Almomin, 2012b), the bulk of work on this topic has concerned linearized extended modeling and related inversion algorithms (Symes and Carazzone, 1991; Chauris and Noble, 2001; Mulder and ten Kroode, 2002; Shen and Symes, 2008; Biondi and Almomin, 2012a; Weibull and Arntsen, 2014, 2013; Shan and Wang, 2013; Shen, 2013; Chauris and Plessix, 2013). An extensive reference list may be found in Symes (2008), where it is argued that these methods address the inverse problem implicitly posed by Migration Velocity Analysis.

Extended modeling relaxes the data fit criterion; a physicality constraint suppresses the non-physical extension. The tension between the two is resolved at a physical model fitting the data. An objective function combining penalties for data misfit and non-physicality would seem an obvious approach to inversion, but contains the data misfit function so is frequency-dependent and just as likely to suffer from spurious local minima as is the standard least-squares objective.

The key to smoothness and unimodality is the *reduced objective*, which comes from a linear inversion for short scale component and depends only on the macro-model (Kern and Symes, 1994; Liu et al., 2013). It is this reduced objective which is smooth, though only for certain choices of physicality constraints (Stolk and Symes, 2003). The reduced objective may also be viewed as an example of variable projection (van Leeuwen and Mulder, 2009). We will use acoustic constant density modeling as an example to illustrate the shape of the reduced objective function and its relation with parameter choices.

EXTENDED MODELING

Denote by $M = \{m(\mathbf{x})\}$ the physical model space and by $\bar{M} = \{\bar{m}(\mathbf{x}, h)\}$ the extended model space, which contains the physical models as a subspace. The variable h is a parameter, such as shot position, offset, ray parameter or parameter vector, subsurface offset, or scattering angle, which characterizes the additional degrees of freedom in the extended model space, over and above position in the subsurface. Denote by D the data space.

Denote by $F : M \mapsto D$ the forward map, or modeling operator, and by $\bar{F} : \bar{M} \mapsto D$ the extended forward map. \bar{F} is an extended modeling operator because for $m \in M$,

$$\bar{F}[m] = F[m].$$

Linearized Extended Waveform Inversion

The abstract basic linearized inverse problem may be formulated: given data $d \in D$, find $m_l, \delta m \in M$ so that

$$DF[m_l]\delta m \simeq d - F[m_l] \quad (1)$$

Here DF denotes the derivative, or Born approximation.

The extended linearized inverse problem is: given d , find $m_l \in M, \delta \bar{m} \in \bar{M}$ so that

$$D\bar{F}[m_l]\delta \bar{m} \simeq d - F[m_l]. \quad (2)$$

REDUCED OBJECTIVE FUNCTION

As mentioned in the introduction, an additional ingredient is needed to drive extended models toward physical (non-extended) models. One approach, by far the most explored, is to introduce an operator which ‘‘measures’’ physicality by mapping physical models to the zero vector, and penalizing the size of its output. Such operators have come to be called *annihilators* (Brandsberg-Dahl et al., 2003).

Thus introduce an operator A on extended model space \bar{M} , satisfying the abstract annihilator property:

$$A\delta m = 0 \text{ for all } \delta m \in M.$$

We will introduce a concrete annihilator in the next section for shot coordinate model extension.

The solution to the basic linearized inverse problem (1) is a solution of the extended linearized inverse problem for which $\delta \bar{m}$ is physical, hence mapped to the zero vector by A . Thus (1) is equivalent to the system

$$\begin{aligned} D\bar{F}[m_l]\delta \bar{m} &\simeq d - F[m_l] \\ A\delta \bar{m} &\simeq 0. \end{aligned} \quad (3)$$

Define:

$$J[m_l, \delta \bar{m}] = \frac{1}{2} \|D\bar{F}[m_l]\delta \bar{m} - (d - F[m_l])\|^2 + \frac{\alpha^2}{2} \|A\delta \bar{m}\|^2, \quad (4)$$

The weight α controls emphasis on physicality: as $\alpha \rightarrow \infty$, the minimizer of $J[m_l, \cdot]$ tends to the solution δm of (1), interpreted as a least squares problem, for fixed m_l, d .

The reduced objective $\bar{J}[m_l]$ is the least value attained by $J[m_l, \delta \bar{m}]$ for any choice of extended model perturbation $\delta \bar{m}$:

$$\bar{J}[m_l] = \min_{\delta \bar{m}} J[m_l, \delta \bar{m}]. \quad (5)$$

Define the normal operator (or Hessian)

$$N[m_l] = D\bar{F}[m_l]^T D\bar{F}[m_l] + \alpha^2 A^T A.$$

Then the minimizer $\delta \bar{m}$ of J may be written as

$$\delta \bar{m} = N[m_l]^{-1} D\bar{F}[m_l]^T (d - F[m_l]). \quad (6)$$

EXAMPLE: EXTENDED 2D CONSTANT DENSITY ACOUSTICS

The simplest useful model for simulation of seismograms is the constant density acoustic wave equation. The model space is a set of velocities, or more conveniently, squared velocities: $M = \{c^2(\mathbf{x})\}$. For this problem, we use shot coordinate \mathbf{x}_s as the extended coordinate and the extended model space is $\bar{M} = \{\bar{c}^2(\mathbf{x}, \mathbf{x}_s)\}$. The pressure field is causal, and solves the constant density acoustic wave equation. The right-hand side represents an isotropic point radiator source with time-dependence $w(t)$:

$$\begin{aligned} \left(\frac{\partial^2}{\partial t^2} - c^2(\mathbf{x}) \nabla_{\mathbf{x}}^2 \right) u(\mathbf{x}, \mathbf{x}_s, t) &= \delta(\mathbf{x} - \mathbf{x}_s) w(t), \\ u(\mathbf{x}, \mathbf{x}_s, t) &= 0, t \ll 0. \end{aligned} \quad (7)$$

The value of both the extended and non-extended forward map for the model $c^2(\mathbf{x})$ is the result of sampling the pressure field at a prescribed set of receiver points for the various source positions in the survey:

$$\bar{F}[c^2] = F[c^2] = \{u(\mathbf{x}_r, \mathbf{x}_s, t)\}.$$

Linearization, or extended Born approximation, results from sampling a pressure field perturbation δu of a background pressure field u_l , the solution of (7) with the background squared velocity $c^2 = c_l^2$, resulting from an extended squared-velocity perturbation $\delta c^2(\mathbf{x}, \mathbf{x}_s)$. Thus the extended Born approximation model space is $M = \{c_l^2(\mathbf{x}), \delta c^2(\mathbf{x}, \mathbf{x}_s)\}$. The perturbational pressure δu solves

$$\begin{aligned} \left(\frac{\partial^2}{\partial t^2} - c_l^2(\mathbf{x}) \nabla^2 \right) \delta u(\mathbf{x}, \mathbf{x}_s, t) &= \delta c^2(\mathbf{x}, \mathbf{x}_s) \nabla^2 u_l(\mathbf{x}, \mathbf{x}_s, t), \\ \delta u(\mathbf{x}, \mathbf{x}_s, t) &= 0, t \ll 0. \end{aligned} \quad (8)$$

So $D\bar{F}[c_l^2]\delta c^2 = \{\delta u(\mathbf{x}_r, \mathbf{x}_s, t)\}$. Note that $D\bar{F}$ is linear in δc^2 , but nonlinear in c_l^2 .

Since physical models do not depend on \mathbf{x}_s , a feasible choice of annihilator for this shot coordinate model extension is (Kern and Symes (1994))

$$A = \frac{\partial}{\partial \mathbf{x}_s}.$$

In fact, as shown by Stolk and Symes (2003), this is essentially the *only* choice of annihilator that will lead to a smooth reduced objective function.

The Marmousi model (Bourgeois et al., 1991) is used in the rest of this abstract. This model is separated into smoothed long scale background model m_l and δm (see figure 1(a), and 1(b)).

The data are computed with 60 shots starting from 3 km, with spacing 100 meters and 12 meters below the sea surface. 96 receivers are placed behind each shot, with offset 200 meters between the first receiver and a shot, 25 meters spacing between each receiver and 8 meters below the surface. We use Ricker wavelet with 10Hz peak frequency as the source. Figure 2 shows the data from 5.8 km shot and 6 km shot. The data is muted and tapered to avoid edge effects.

Linearized Extended Waveform Inversion

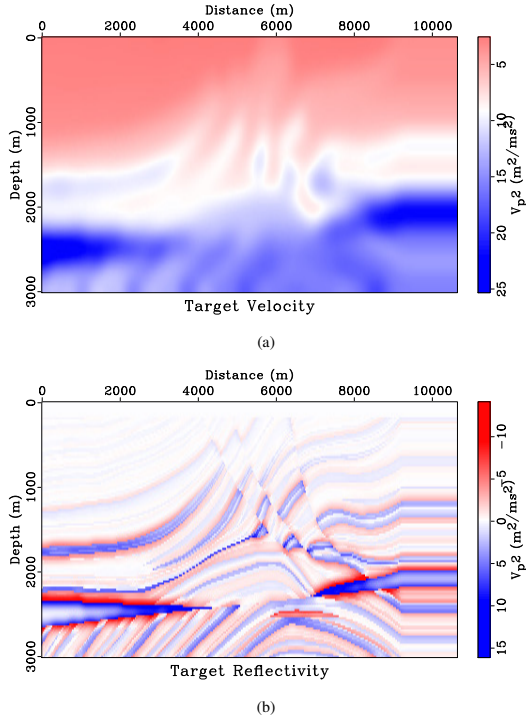


Figure 1: (a) smoothed Marmousi model m_l . (b) δm the reflectivity.

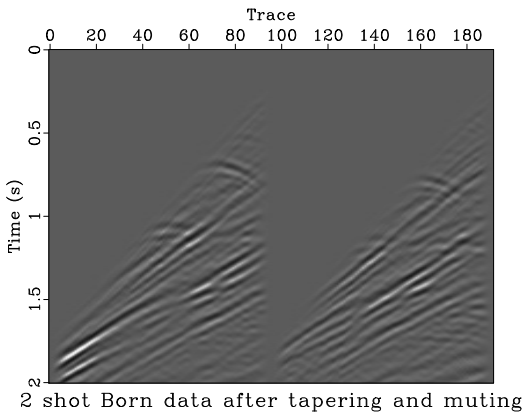


Figure 2: Data is computed using the true velocity and reflectivity as in figure 1(a) and 1(b) with $x_s = 5.8 \text{ km}, 6 \text{ km}$. Data shown in this figure has been applied tapering and muting.

The extended approach to inversion draws inspiration from migration velocity analysis. In principle, migrated shot record image volumes should be "flat" along the shot axis, i.e. independent of x_s for correct velocity. In practice, amplitude anomalies may obscure this effect, as is illustrated in figure 3(a)

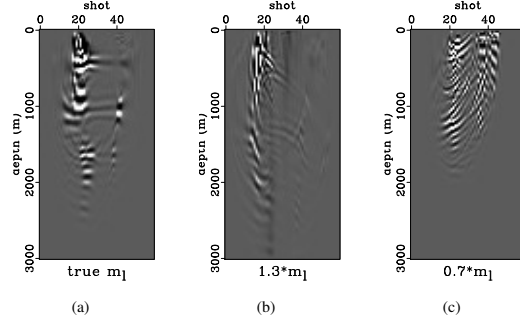


Figure 3: RTM image gathers for (a) right velocity, (b) 1.3 times of right velocity, (c) 0.7 times of right velocity at $x = 5088\text{m}$.

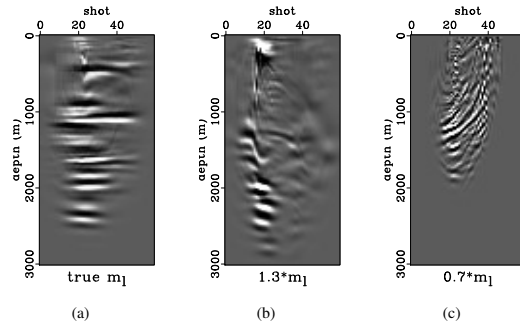


Figure 4: Inversion image gathers for (a) right velocity, (b) 1.3 times of right velocity, (c) 0.7 times of right velocity for $\alpha = 0.01$.

Instead, we follow the mathematical path laid out above, and base our construction of an objective function on the linearized inversion volume ($\delta \bar{m}$, solution of equation (6), instead of the migrated image volume. We use conjugate gradient iteration (Nocedal and Wright, 1999) to approximately minimize $J[m_l, \delta \bar{m}]$ over $\delta \bar{m}$, solve the normal equation (6) and thus compute $\bar{J}[m_l]$ (equation 5).

Figure 4 shows image (z, x_s) gathers for the same horizontal position as in figure 3. We use weight $\alpha = 0.01$, and perform 100 conjugate gradient iterations. The gradient (normal residual) is reduced 5% of its original value for the true low frequency velocity, and 9% of its original value for other velocities. We can see clearly the flatness of the inverted gathers for correct velocity, and the systematic tendency to slope one way or the other when the velocity is incorrect.

Increasing α will force the inverted velocity to be more x_s -independent, and the objective to behave more like the ordinary least-squares objective. Figure 5 shows the same image gathers as figure 4, but this time with $\alpha = 0.1$. Now the

Linearized Extended Waveform Inversion

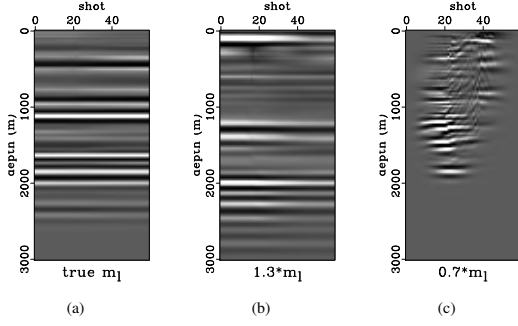


Figure 5: Inversion image gathers for (a) right velocity, (b) 1.3 times of right velocity, (c) 0.7 times of right velocity for $\alpha = 0.1$.

requirement of \mathbf{x}_s -independent has largely overwhelmed the kinematic information in the gathers.

Figure 6 displays the values of the approximate $\tilde{J}[m]$ along the line segment

$$m = \sigma m_l,$$

with 11 evenly spaced points of $\sigma \in [0.6, 1.4]$, for several values of α (0.01, 0.1, and 1.0), and less (20 iterations) and more (100 iterations) application of the conjugate gradient algorithm. Here m_l is the background velocity displayed in Figure 1(a). Small α tends to give flat valley near the global minimum, while with large α , the valley is deep and narrow, and stationary points other than global minima appear.

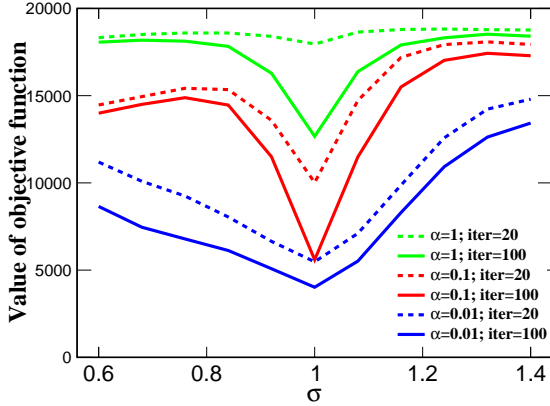


Figure 6: Values of $\tilde{J}[m]$ for $m = \sigma m_l$ with $\sigma \in [0.6, 1.4]$: several values of α , and 20 or 100 conjugate gradient iterations.

Figure 7 shows a similar sampling of $\tilde{J}[m]$ values for the line segment

$$m = (1 - \sigma)m_l + \sigma m_0, \quad m_0(\mathbf{x}) = 1500 \text{m/s}$$

with 11 evenly spaced choices of $\sigma \in [-0.4, 0.6]$.

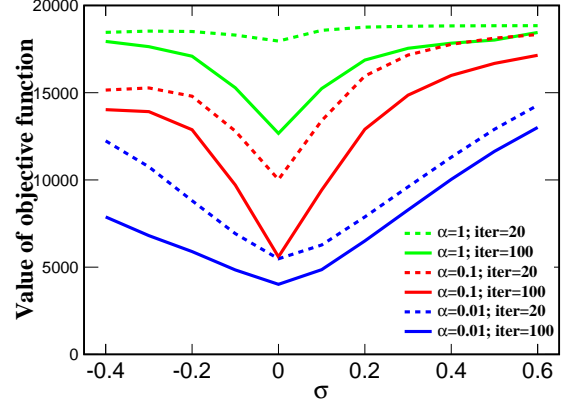


Figure 7: Values of $\tilde{J}[m]$ for $m = (1 - \sigma)m_l + \sigma m_0$ with $\sigma \in [-0.4, 0.6]$ and $m_0 = 1500$ m/ms: several values of α , and 20 or 100 conjugate gradient iterations.

CONCLUSION

A natural objective function for the linearized extended waveform inversion combines least squares data misfit and a differential semblance penalty for non-physical dependence on the model extension coordinates. We have examined this objective for constant density acoustic modeling of reflected waves. As suggested by Kern and Symes (1994), the reduced objective (with short scale components eliminated via a quadratic optimization) tends to be smooth and unimodal in the background (velocity) model parameters, with proper choice of penalty weight and sufficiently precise solution of the inner minimization. Stolk and Symes (2003) showed that the reduced objective has these properties only for the differential measure of semblance, up to inessential modifications.

This conclusion suggests two important topics for further work. First, the choice of penalty weight is obviously critical, and an objective criterion for that choice is needed. One possible approach to setting α lies in recognizing its identity as a Lagrange multiplier: it is possible to recast the extended waveform inversion problem as the minimization of the differential semblance penalty subject to a bound on mean-square data error, and a value for the latter implies a choice of α , which varies in a systematic way as the optimization proceeds. A second area for further work is reduction in the cost of the inner iteration (a version of least squares migration). Preconditioned Krylov space methods seem natural for this problem, and many preconditioners have been suggested in the recent literature. It remains to evaluate them in the context of extended waveform inversion.

ACKNOWLEDGMENTS

We wish to thank the sponsors of The Rice Inversion Project for their continued support.

Linearized Extended Waveform Inversion

REFERENCES

- Biondi, B., and A. Almomin, 2012a, Tomographic full waveform inversion by combining full waveform inversion with wave equation migration velocity analysis: SEG 2012 Annual Meeting, SEG, Expanded Abstracts.
- , 2012b, Tomographic full waveform inversion (TFWI) by combining full waveform inversion with wave-equation migration velocity analysis: 82nd Annual International Meeting, Expanded Abstracts, Society of Exploration Geophysicists, SI9.5.
- Bourgeois, A., P. Lailly, and R. Versteeg, 1991, The Marmousi model, *in* The Marmousi Experience: IFP/Technip.
- Brandsberg-Dahl, S., M. V. De Hoop, and B. Ursin, 2003, Focusing in dip and ava compensation on scattering-angle/azimuth common image gathers: *Geophysics*, **68**, 232–254.
- Chauris, H., and M. Noble, 2001, Two-dimensional velocity macro model estimation from seismic reflection data by local differential semblance optimization: applications synthetic and real data sets: *Geophysical Journal International*, **144**, 14–26.
- Chauris, H., and R.-E. Plessix, 2013, Differential waveform inversion - a way to cope with multiples?: 75th EAGE Conference and Exhibition, Expanded Abstracts.
- Gauthier, O., A. Tarantola, and J. Virieux, 1986, Two-dimensional nonlinear inversion of seismic waveforms: *Geophysics*, **51**, 1387–1403.
- Jannane, M., W. Beydoun, E. Crase, D. Cao, Z. Koren, E. Landa, M. Mendes, A. Pica, M. Noble, G. Roeth, S. Singh, R. Snieder, A. Tarantola, D. Trezeguet, and M. Xie, 1989, Wavelengths of earth structures that can be resolved from seismic reflection data: *Geophysics*, **54**, 906–910.
- Kern, M., and W. W. Symes, 1994, Inversion of reflection seismograms by differential semblance analysis: Algorithm structure and synthetic examples: *Geophysical Prospecting*, **99**, 565–614.
- Liu, Y., W. Symes, Y. Huang, and Z. Li, 2013, Linearized extended waveform inversion via differential semblance optimization in the depth-oriented extension: SEG 2013 Annual Meeting, SEG, Expanded Abstracts.
- Mulder, W. A., and A. P. E. ten Kroode, 2002, Automatic velocity analysis by differential semblance optimization: *Geophysics*, **67**, 1184–1191.
- Nocedal, J., and S. Wright, 1999, *Numerical Optimization*: Springer Verlag.
- Santosa, F., and W. W. Symes, 1989, An Analysis of Least-Squares Velocity Inversion: Society of Exploration Geophysicists, volume 4 of *Geophysical Monographs*.
- Shan, G., and Y. Wang, 2013, RTM based wave equation migration velocity analysis: SEG 2013 Annual Meeting, SEG, Expanded Abstracts, 4726–4731.
- Shen, P., 2013, An rtm based automatic migration velocity analysis in image domain: SEG 2012 Annual Meeting, SEG, Expanded Abstracts.
- Shen, P., and W. W. Symes, 2008, Automatic velocity analysis via shot profile migration: *Geophysics*, **73**, VE49–60.
- Stolk, C. C., and W. W. Symes, 2003, Smooth objective functionals for seismic velocity inversion: *Inverse Problems*, **19**, 73–89.
- Symes, W. W., 1986, Stability and instability results for inverse problems in several-dimensional wave propagation, *in* Proc. 7th International Conference on Computing Methods in Applied Science and Engineering: North-Holland.
- , 1991, Layered velocity inversion: a model problem from reflection seismology: *SIAM Journal on Mathematical Analysis*, **22**, 680–716.
- , 2008, Migration velocity analysis and waveform inversion: *Geophysical Prospecting*, **56**, 765–790.
- Symes, W. W., and J. J. Carazzone, 1991, Velocity inversion by differential semblance optimization: *Geophysics*, **56**, 654–663.
- van Leeuwen, T., and W. A. Mulder, 2009, A variable projection method for waveform inversion: Presented at the 71st Conference EAGE, European Association for Geoscientists and Engineers. (Expanded Abstract).
- Virieux, J., and S. Operto, 2009, An overview of full waveform inversion in exploration geophysics: *Geophysics*, **74**, WCC127–WCC152.
- Weibull, W. W., and B. Arntsen, 2013, Automatic velocity analysis with reverse time migration: *Geophysics*, **78**, S179–S192.
- , 2014, Anisotropic migration velocity analysis using reverse time migration: *Geophysics*, **79**, R13–R25.